Journal of the American College of Cardiology
© 2004 by the American College of Cardiology Foundation
Published by Elsevier Inc.

Vol. 44, No. 11, 2004
ISSN 0735-1097/04/$30.00
doi:10.1016/j.jacc.2004.08.057

Mechanical Unloading Improves Intracellular Ca^{2+} Regulation in Rats With Doxorubicin-Induced Cardiomyopathy

Tohru Takaseya, MD,* Masaru Ishimatsu, MD, PHD,† Eiki Tayama, MD, PHD,*
Akinori Nishi, MD, PHD,† Takashi Akasu, MD, PHD,† Shigeaki Aoyagi, MD, PHD*
Kurume, Japan

OBJECTIVES We sought to assess whether mechanical unloading has beneficial effects on cardiomyocytes from doxorubicin-induced cardiomyopathy in rats.

BACKGROUND Mechanical unloading by a left ventricular assist device (LVAD) improves the cardiac function of terminal heart failure in humans. However, previous animal studies have failed to demonstrate beneficial effects of mechanical unloading in the myocardium.

METHODS The effects of mechanical unloading by heterotopic abdominal heart transplantation were evaluated in the myocardium from doxorubicin-treated rats by analyzing the intracellular free calcium level ($[Ca^{2+}]_i$) and the levels of intracellular Ca^{2+}-regulatory proteins.

RESULTS In doxorubicin-treated rats, the duration of cell shortening and $[Ca^{2+}]_i$ transients in cardiomyocytes was prolonged (432 ± 28.2% of control in 50% relaxation time; 184 ± 10.5% of control in $[Ca^{2+}]_i$ 50% decay time). Such prolonged time courses significantly recovered after mechanical unloading (114 ± 10.4% of control in 50% relaxation time; 114 ± 5.8% of control in 50% decay time). These effects were accompanied by an increase in sarcoplasmic reticulum Ca^{2+} ATPase (SERCA2a) protein levels (0.97 ± 0.05 in unloaded hearts vs. 0.41± 0.09 in non-unloaded hearts). The levels of other intracellular Ca^{2+}-regulatory proteins (phospholamban and ryanodine receptor) were not altered after mechanical unloading in doxorubicin-treated hearts. These parameters in unloaded hearts without doxorubicin treatment were similar to normal hearts.

CONCLUSIONS Mechanical unloading increases functional sarcoplasmic reticulum Ca^{2+} ATPase and improves $[Ca^{2+}]_i$ handling and contractility in rats with doxorubicin-induced cardiomyopathy. These beneficial effects of mechanical unloading were not observed in normal hearts. (J Am Coll Cardiol 2004;44:2239–46) © 2004 by the American College of Cardiology Foundation

Mechanical unloading of end-stage failing hearts with the left ventricular assist device (LVAD) in humans improves cardiac function (1–8). In some cases (1), the LVAD can eventually be explanted (bridge to recovery) and heart transplantation is no longer necessary. On the other hand, animal studies failed to prove the beneficial effects of mechanical unloading of hearts. Ito et al. (9) have reported that mechanical unloading applied to a normal rat heart leads to less myocardial contractility, accompanied by a depressed sarcoplasmic reticulum (SR) Ca^{2+} ATPase (SERCA2a)/phospholamban ratio. Other previous studies using animals have shown that unloading produces an atrophic heart, along with decreased protein synthesis (10), reactivated fatal genes (11), and alterations in membrane Ca^{2+} transport mechanisms (12–14). Ritter et al. (15) reported that the decay of intracellular free Ca^{2+} level ($[Ca^{2+}]_i$) transients and SR Ca^{2+} adenosine triphosphatase (ATPase, or SERCA2a) function were not altered in the atrophic heart induced by mechanical unloading. Results from these animal studies have shown that the mechanism of mechanical unloading, which improves cardiac function of a failing heart in the human, is unclear. These previous studies investigated the effects of mechanical unloading on the normal heart (9–15). Although the LVAD is implanted in humans with terminal heart failure, there is no evidence from animal studies that shows any beneficial effects or the mechanism of unloading in the failing myocardium. Doxorubicin is known to induce cardiomyopathy by reducing SERCA2a messenger ribonucleic acid (mRNA) levels and results in impaired $[Ca^{2+}]_i$ handling (16). In this study, we explored whether mechanical unloading via heterotopic heart transplantation improved $[Ca^{2+}]_i$ regulation in rats with doxorubicin-induced cardiomyopathy.

METHODS

Experimental design. This study was carried out in accordance with the Guide for Animal Experimentation, Kurume University. The experimental design is summarized in a flow chart (Fig. 1).

Doxorubicin-induced cardiomyopathy model. Doxorubicin-induced cardiomyopathy was generated as previously described (17,18). Male LEW/Crj rats (six weeks old) weighing 180 to 220 g were used. Doxorubicin hydrochloride (D1515, Sigma, St. Louis, Missouri) was administered intraperitoneally in six equal injections (each containing 2.5 mg/kg) over a period of two weeks, with a total cumulative dosage of 15 mg/kg body weight (18). For control animals, saline (0.4 ml) was injected in the same manner.

From the Departments of *Surgery and †Physiology, Kurume University School of Medicine, Kurume, Japan.

Manuscript received May 28, 2004; revised manuscript received August 5, 2004, accepted August 23, 2004.

JACC Vol. 44, No. 11, 2004
December 7, 2004:2239–46

Abbreviations and Acronyms

$[Ca^{2+}]_i$	= intracellular free Ca^{2+} level
GAPDH	= glyceraldehyde-3-phosphate dehydrogenase
LV	= left ventricle/ventricular
LVAD	= left ventricular assist device
PLB	= phospholamban
RT-PCR	= reverse transcription-polymerase chain reaction
RyR	= ryanodine receptor
SERCA2a	= sarcoplasmic reticulum Ca^{2+} adenosine triphosphatase (ATPase)
SR	= sarcoplasmic reticulum

Mechanical unloading model. Mechanical unloading was brought about by heterotopic heart transplantation. In this model, there is intact perfusion but limited chamber filling in the left ventricle (LV) of the implanted heart, which significantly reduces its workload. Two weeks after the final doxorubicin or saline injection, the rat was anesthetized with sodium pentobarbital (40 mg/kg intraperitoneally). The heart was then arrested by infusion of cardioplegia containing (in mmol/l): NaCl 110, $NaHCO_3$ 10, KCl 16, $MgCl_2$ 16, $CaCl_2$ 1.2, and lidocaine 1.0. The heart was then removed and transplanted into the abdomen of an inbred recipient rat under sodium pentobarbital (40 mg/kg intraperitoneally) (19) by joining the donor ascending aorta to the recipient abdominal aorta, as well as the donor pulmonary artery to the recipient inferior vena cava in an end-to-side fashion. The ischemic time was ~40 min. The transplanted heart was resuscitated to spontaneous continuous beating after restoration of coronary blood flow. The recipients were killed, and the transplanted heart was removed two weeks later.

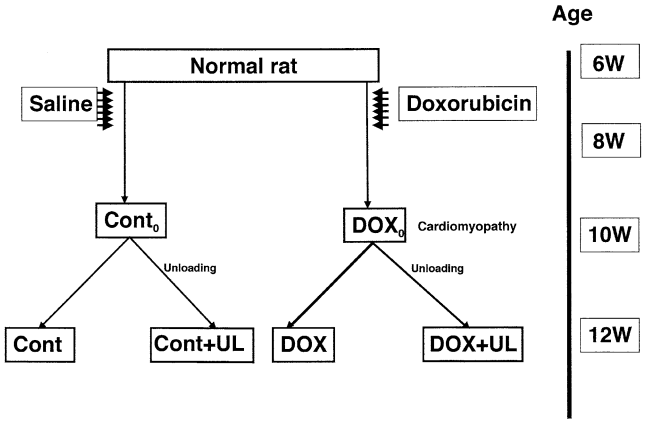

Figure 1. Experimental design. Normal rats (6 weeks old) were divided into two groups, control group (intraperitoneal administration of 0.4 ml saline 6 times in 2 weeks) and doxorubicin-treated group (intraperitoneal administration of 2.5 mg/kg body weight 6 times in 2 weeks). Two weeks after the final injection, each group was further divided into two groups according to with or without heterotopic heart transplantation (the heart of each group was transplanted into age-matched normal rat abdomen). $Cont_0$ = control group two weeks after the final intraperitoneal injection; DOX_0 = doxorubicin-treated group two weeks after the final intraperitoneal injection; Cont = control group four weeks after the final intraperitoneal injection; DOX = doxorubicin-treated group four weeks after the final intraperitoneal injection; Control+UL = the heart from the control group, which was applied unloading for two weeks; DOX+UL = the heart from the doxorubicin-treated group, which was applied unloading for two weeks. Cont+UL was compared with Cont to evaluate the effects of mechanical unloading on normal hearts; DOX+UL was compared with DOX to evaluate the effects of unloading on the failing myocardium. All four groups (Cont, Cont+UL, DOX, and DOX+UL) were age-matched at the time of in vitro analysis.

Cardiomyocyte isolation. Isolation of LV cardiomyocytes from rats was performed as previously described (20). Briefly, hearts were excised from rats, which were deeply anesthetized with pentobarbital sodium (100 mg/kg intraperitoneally). Hearts were mounted on a Langendorff perfusion apparatus. After perfusion for 5 min at 37°C at a pressure of 80 to 100 mm Hg with Ca^{2+}-free Tyrode's solution containing (in mmol/l): NaCl 140, KCl 4, $MgCl_2$ 1, $NaHCO_3$ 18, D-glucose 11, HEPES 10, and insulin 0.13 U/ml (pH 7.4), the perfusate solution was switched to the same solution with 0.8 mg/ml collagenase (type I, Sigma C-0130) and 0.2 mmol/l $CaCl_2$ until the heart became flaccid (7 to 10 min). The ventricular tissue was then removed and incubated in Tyrode's solution containing 0.5 mmol/l $CaCl_2$ with 0.8 mg/ml collagenase at 37°C for 20 min. Ventricular tissue was dispersed, filtered, and suspensions were rinsed several times (gradually increasing $[Ca^{2+}]$ to 1.0 mmol/l).

Only cells that were rod shaped without blebs or other morphologic alterations were used for the study. Isolated cardiomyocytes were stored in Dulbecco's modified Eagle's medium (Life Technologies, Rockville, Maryland) supplemented with 25 mmol/l HEPES at 37°C and used in the experiments within 6 h after isolation.

Measurement of cell shortening and $[Ca^{2+}]_i$ transients. Cell shortening and transient change in $[Ca^{2+}]_i$ were measured sequentially in the same myocyte. The dye solution was prepared as follows: 50 μg of Oregon Green was first added to 4 μl of dimethyl sulfoxide (DMSO) and 2 μl of 20% pluronic (Molecular Probes) and then diluted with Ca^{2+}-free Tyrode's solution to a final concentration of 10 μmol/l. The cells were treated with 1 ml of dye solution for 60 min at 37°C. After dye treatment, myocytes were washed twice in Tyrode's solution and then seeded to a glass-bottom recording chamber under an uplight microscope (Axioscop 2 FS, Zeiss, Germany) equipped with an OZ/Intervision laser scanning confocal microscope (Noran Instruments, Middleton, Wisconsin). Cells were illuminated by excitation light (at 488 nm), and emission fluorescence (at >515 nm) was captured through a barrier filter. Fluorescent images (512 × 60 pixels) were captured by band scan for 2 s at 4 ms/flame (240 fps) at a trial. Five trials per cardiomyocyte were repeated to average images. All imaged data were stored in an UNIX-based computer (O2, Silicon Graphics, Inc., Mountain View, California). The intensity of fluorescence from a region of interest (40 × 10 pixels) was averaged. Because the initial value of the intensity varied among the cells, F/F0 was used, where F0 is the mean resting value that was obtained just before electrical stimulation, and F is the obtained value. The isolated cardiomyocyte was then stimulated electrically (0.2 ms in

Table 1. Body and LV Weight

	Control	Control + UL	DOX	DOX + UL
n (hearts)	16	14	16	13
Body weight (g)	386 ± 26	—	287 ± 16*	—
LV weight (mg)	680 ± 34	352 ± 29*	480 ± 34*	330 ± 26†
LVW/BW (mg/g)	1.76 ± 0.6	—	1.67 ± 0.4	—

*$p < 0.05$ vs. control.†$p < 0.05$ vs. DOX. Data are presented as the mean value ± SEM.
LV = left ventricular; LVW/BW = ratio of left ventricular weight to body weight; UL = unloaded.

duration, 1 Hz) using bipolar platinum electrodes placed close to the cell. During recording, the cells were superfused at 2 ml/min with Tyrode's solution containing Ca^{2+} (1.8 mmol/l) at 37°C.

Fluorescent images were also evaluated for cell shortening analysis. The change of cell length by electrical stimulation was measured using Image-J software (National Institute of Mental Health, Bethesda, Maryland). Fractional cell shortening was calculated as: [1 − (systolic length/diastolic length)] × 100 (%). V_{max} was determined as $(d [Ca^{2+}]_i/dt)_{max}$ to evaluate the maximal slope of the rising phase of $[Ca^{2+}]_i$ transients.

Messenger RNA isolation and quantitative real-time reverse transcription polymerase chain reaction (RT-PCR). Total RNA from the deep-frozen apex of the LV tissue was prepared using an RNA kit (Qiagen, Hilden, Germany). The RNA integrity was checked electrophoretically and quantified spectrophotometrically. Complementary DNA (cDNA) was transcribed from the RNA template using Sensiscript Reverse Transcriptase (Qiagen, Hilden, Germany) and Oligo-dT primers (Gibco BRL, Karlsruhe, Germany).

Real-time RT-PCR was performed in the Light-Cycler PCR and detection system (Roche, Mannheim, Germany) using the Reaction Mix SYBR Green I kit (Roche Molecular Biochemicals), as previously described (21). The primer pairs used for RT-PCR were as follows: for glyceraldehyde-3-phosphate dehydrogenase (GAPDH), sense primer: 5′-CTTCACCACCATGGAGAAGGC-3′ (338–358 base pair [bp]) and anti-sense primer: 5′-GGCATGGACTGTGGTCATGAG-3′ (575–545 bp, by GeneBank Accession AB017801); for SERCA2a, sense primer: 5′-AAGCCACAGAGACTGCTCTCAC-3′ (1523–1544 bp) and anti-sense primer: 5′-CGCAGAATCTTCCAGGTGCATC-3′ (1950–1929 bp, by GeneBank Accession X15635); and for ryanodine receptor (RyR), sense primer: 5′-AGAGAAGGAAGTGGCACGGAA-3′ (835–855 bp) and anti-sense primer: 5′-GAAGCCCATCGCGATGTCAAG-3′ (1279–1259 bp, by GeneBank Accession U95157). The expected amplified fragment lengths for SERCA2a, RyR, and GAPDH were 428, 445, and 238 bp, respectively.

Fluorescence-labeled light cycler probes annealed to the homologous sequences in close proximity, enabling fluorescence energy transfer between the donor and the acceptor dye to be measured during the annealing step. The SYBR Green I preferentially bound to dsDNA that was generated. Melting curves, which were analyzed immediately after amplification, revealed the characteristic melting peaks that allowed the differentiation of specific from nonspecific products such as primer dimers.

Western blot analysis of SERCA2a, RyR, and phospholamban (PLB) protein levels. In rats, the hearts were excised, and the LV tissue was frozen in liquid nitrogen and stored at −80°C until use. Tissue was sonicated in 1 ml of 1% sodium dodecyl sulfate, and equal amounts of total protein (5 or 50 μg/lane) were separated by a 6% or 14% sodium dodecyl sulfate-polyacrylamide gel. Separated proteins were transferred to a nitrocellulose membrane (Schleicher & Schuell, Keene, New Hampshire). Membranes were immunoblotted with anti-SERCA2a monoclonal antibody (1:250; Santa Cruz Biotechnology, Inc., Santa Cruz, California), anti-PLB antibody (1:500; Affinity Bioreagents, Golden, Colorado), anti-RyR antibody (1:500; Af-

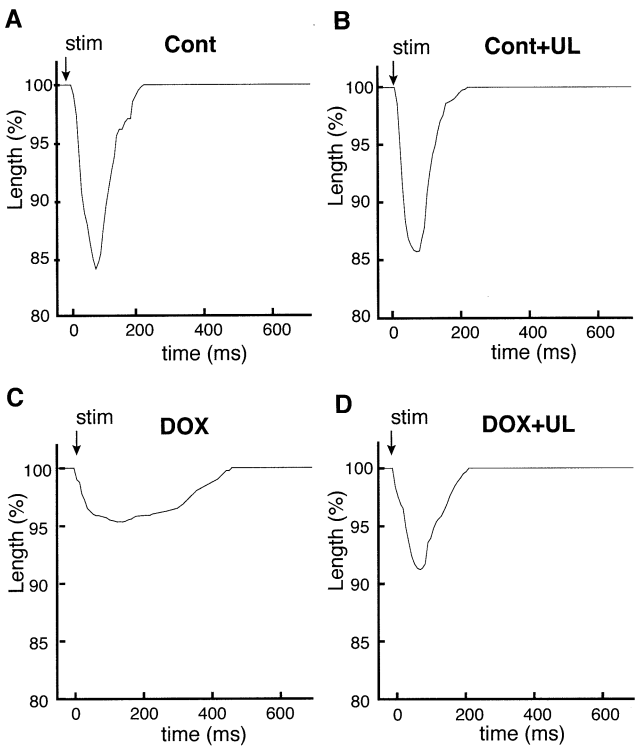

Figure 2. Representative traces of cell shortening in isolated cardiomyocytes from four groups, evoked by electrical stimulation under perfusion conditions of 37°C, $[Ca^{2+}]_0$ was 1.8 mmol/l, and the pacing rate was 1.0 Hz. The electrical stimulation was applied at the arrow. **(A)** Cont. **(B)** Cont+UL. **(C)** DOX. **(D)** DOX+UL. Note that the time courses of cell shortening and relaxation are extremely prolonged in DOX and have recovered in DOX+UL. Abbreviations as in Figure 1.

Table 2. Indexes of Cell Shortening

	Control	Control + UL	DOX	DOX + UL
n (cells)	27	24	26	26
Time to peak shortening (ms)	64.6 ± 5.1	66.7 ± 5.3	135 ± 8.9*	85.0 ± 7.8†
	100	(103 ± 8.2)	(210 ± 13.8)	(132 ± 12.1)
50% relaxation time (ms)	49.2 ± 3.4	42.6 ± 4.0	213 ± 13.9*	56.3 ± 5.1†
	100	(86.6 ± 8.1)	(432 ± 28.2)	(114 ± 10.4)
90% relaxation time (ms)	112 ± 10.9	106 ± 11.1	305 ± 24.6*	117 ± 11.8†
	100	(93.8 ± 9.7)	(271 ± 21.9)	(104 ± 10.5)
Fractional cell shortening (%)	15.9 ± 0.9	14.4 ± 1.1	4.7 ± 0.3*	8.6 ± 0.5†
	100	(90.6 ± 6.9)	(29.6 ± 1.9)	(54.1 ± 3.1)

*$p < 0.05$ vs. control.†$p < 0.05$ vs. DOX. Data are presented as the mean value ± SEM. Normalized values (%) versus control are indicated in parentheses.
Abbreviations as in Table 1.

finity Bioreagents), and anti-GAPDH antibody (1:500; Santa Cruz) at room temperature for 2 h. Antibody binding was revealed by incubation with donkey anti-goat Alexa Fluor 680-linked immunoglobulin G, goat anti-mouse Alexa Fluor 680-linked immunoglobulin G, or goat anti-rabbit Alexa Fluor 680-linked immunoglobulin G (1:5000, Molecular Probes, Inc., Eugene, Oregon) for 30 min. The membranes were scanned and quantified with the Odyssey Infrared Imaging System (LI-COR). Samples from four groups were analyzed on individual immunoblots. For each experiment, values obtained for control+unloaded (UL), doxorubicin (DOX), and DOX+UL were calculated relative to the value for the control.

Ultrastructural studies. For ultrastructural studies, five hearts in each group were processed as previously described (18,22). Hearts were washed in cold 0.1-mol/l sodium phosphate buffer (pH 7.4). A tissue sample of 1 to 2 mm in size was taken from the apex of the heart. The minced tissue was immersed in 0.1-mol/l phosphate buffer (pH 7.4) containing 2% glutaraldehyde for 2 h. The tissue was washed for 1 h in the above phosphate buffer containing 50-mmol/l sucrose. Post-fixation was done in 2% osmium tetroxide for 2 h. Tissue embedding was done in Quetol 812 (Nisshin EM, Tokyo, Japan). Ultra-thin sections were stained with lead citrate, and these were examined using a Hitachi H-7000 transmission electron microscope (Hitachi, Tokyo, Japan).

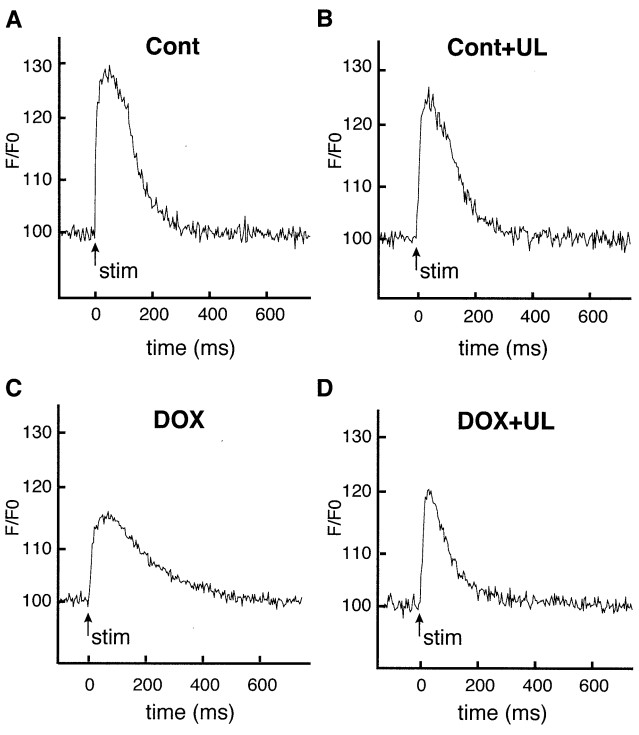

Figure 3. Representative traces of $[Ca^{2+}]_i$ transients in isolated cardiomyocytes from four groups, evoked by electrical stimulation under perfusion conditions of 37°C. $[Ca^{2+}]_0$ was 1.8 mmol/l and pacing rate was 1.0 Hz. The electrical stimulation (stim) was applied at the **arrow**. **(A)** Cont. **(B)** Cont+UL. **(C)** DOX. **(D)** DOX+UL. Abbreviations as in Figure 1.

Statistical analysis. All data are expressed as the mean value ± SEM. A statistical comparison of the data was performed using analysis of variance followed by Bonferroni's all pair's comparison (6 pairs from 4 groups) for individual significant differences. All statistical analyses were performed using the Kaleida Graph version 3.6 (Synergy Software, Reading, Pennsylvania), and Bonferroni's adjusted p value; $p < 0.05$ was considered statistically significant.

RESULTS

Body and LV weight. All rats survived until two weeks after the final doxorubicin injection. From two to four weeks after a final doxorubicin injection, the mortality rate was 21.6% (21 of 97). The rats that survived four weeks after the final doxorubicin injection showed an enlarged abdomen, ascites, and a turgid liver and appeared weaker and lethargic. The heart was removed from control (Cont) or doxorubicin-treated rats two weeks after the final saline or doxorubicin injection ($Cont_0$ or DOX_0) and transplanted into an abdomen of an inbred normal recipient rat for mechanical unloading. Two weeks after the transplantation, each transplanted heart maintained spontaneous heart beats (>200 beats/min).

Table 1 shows the body weight (BW) and LV weight (LVW) and their ratios (Fig. 1). The LV weighed less in DOX than control by 71%, but the LVW/BW ratio was not significantly different. The LV weights in unloaded groups with or without doxorubicin treatment were less than those in DOX or control groups (69% in DOX+UL; 52% in control + UL). Because the unloaded heart was implanted

Table 3. Indexes of $[Ca^{2+}]_i$ Transient

	Control	Control + UL	DOX	DOX + UL
n (cells)	27	24	26	26
Time to peak $[Ca^{2+}]_i$ (ms)	43.3 ± 4.1	51.0 ± 5.8	77.7 ± 5.1*	51.9 ± 6.1†
	100	(118 ± 17.4)	(179 ± 15.3)	(120 ± 18.3)
Peak value of $[Ca^{2+}]_i$ (F/F0)	130 ± 3.9	129 ± 4.3	118 ± 2.0	125 ± 1.8
	100	(99.2 ± 3.3)	(90.8 ± 1.5)	(96.2 ± 1.4)
50% decay time in $[Ca^{2+}]_i$ (ms)	86.1 ± 6.4	103 ± 6.9	158 ± 9.0*	97.7 ± 5.0†
	100	(119 ± 8.0)	(184 ± 10.5)	(114 ± 5.8)
90% decay time in $[Ca^{2+}]_i$ (ms)	194 ± 8.6	239 ± 14.0	408 ± 28.4*	257 ± 34.7†
	100	(123 ± 7.2)	(210 ± 14.6)	(133 ± 17.8)
V_{max} (%/s)	15.2 ± 2.7	10.2 ± 2.2*	7.7 ± 1.4*	9.3 ± 1.8
	100	(67.1 ± 14.5)	(50.7 ± 9.2)	(61.2 ± 11.8)

*$p < 0.05$ vs. control.†$p < 0.05$ vs. DOX. Data are presented as the mean value ± SEM. Normalized values (%) versus control are indicated in parentheses.

Abbreviations as in Table 1.

in the recipient rat, the LVW/BW ratio could not be measured. In order to evaluate the effects of mechanical unloading in cardiomyopathic rats, we compared unloaded hearts (DOX+UL) with hearts without unloading (DOX) after the final doxorubicin injection.

Cell shortening and $[Ca^{2+}]_i$ transients. First, we observed characteristics of isolated cell shortening. Figure 2 shows representative traces of cell shortening, and Table 2 shows indexes measured from cell shortening and relaxation. There were no significant differences in any of the indexes between control and control+UL. The fractional cell shortening of DOX was significantly smaller than that of control, although it was restored after mechanical unloading (DOX+UL). All the indexes of shortening and relaxation in DOX were significantly longer than those in control, but the prolonged indexes recovered in DOX+UL. Although mechanical unloading did not change contractility in the normal cardiomyocytes, the contractility from rats with doxorubicin-induced cardiomyopathy was improved after mechanical unloading. We then measured $[Ca^{2+}]_i$ transients because intracellular free Ca^{2+} is the key messenger in contractile function of cardiomyocytes.

Figure 3 shows representative traces of $[Ca^{2+}]_i$ transients, and Table 3 shows characteristic indexes from $[Ca^{2+}]_i$ transients. The indexes of $[Ca^{2+}]_i$ transients from control+UL were virtually identical to those of control, except for V_{max}. The peak amplitude of the $[Ca^{2+}]_i$ transient was slightly lower in DOX; however, there was no significant difference in the four groups. The time to peak of $[Ca^{2+}]_i$ transients from DOX was longer than that of control; however, it was shortened in myocytes from DOX+UL. Moreover, the 50% and 90% decay times in $[Ca^{2+}]_i$ transients were significantly prolonged in myocytes from DOX compared with control, but the prolonged durations recovered after unloading (DOX+UL). As a result, the steady phase in $[Ca^{2+}]_i$ transients followed by a decline phase in control was hardly observed in DOX (Figs. 3A and 3C). The steady phase could be observed in DOX+UL (Fig. 3D). The characteristics of cell shortening and $[Ca^{2+}]_i$ transients in myocytes from $Cont_0$ or DOX_0 were similar to those of the control or DOX (data not shown). These data suggest that the myocytes from doxorubicin-induced cardiomyopathy rats have depressed contractility accompanied by a slow $[Ca^{2+}]_i$ transient. Such

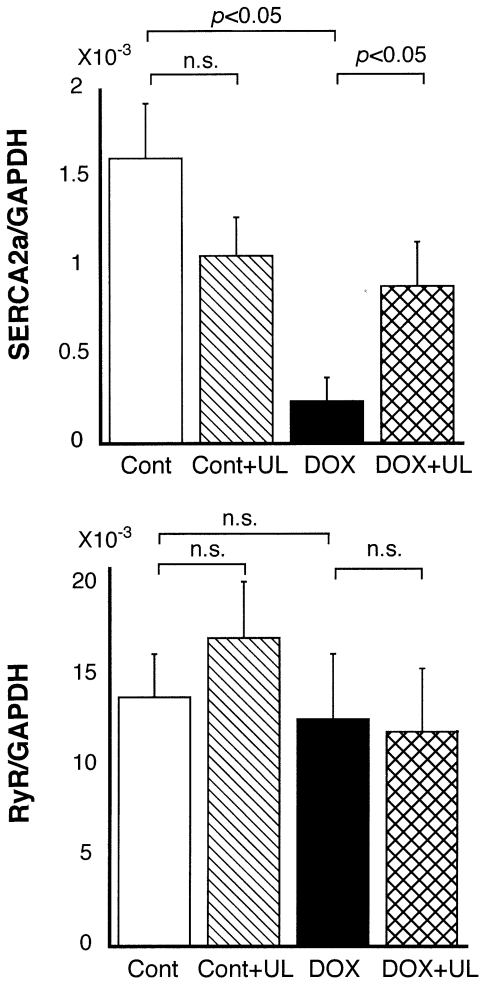

Figure 4. Summary of sarcoplasmic reticulum Ca^{2+} adenosine triphosphatase (SERCA2a)/glyceraldehyde-3-phosphate dehydrogenase (GAPDH) and ryanodine receptor (RyR)/GAPDH mRNA levels. The expression levels of SERCA2a and RyR mRNA were not changed in the Cont and Cont+UL groups. The expression levels of SERCA2a mRNA had recovered in the DOX+UL groups, with no change in RyR levels. Other abbreviations as in Figure 1.

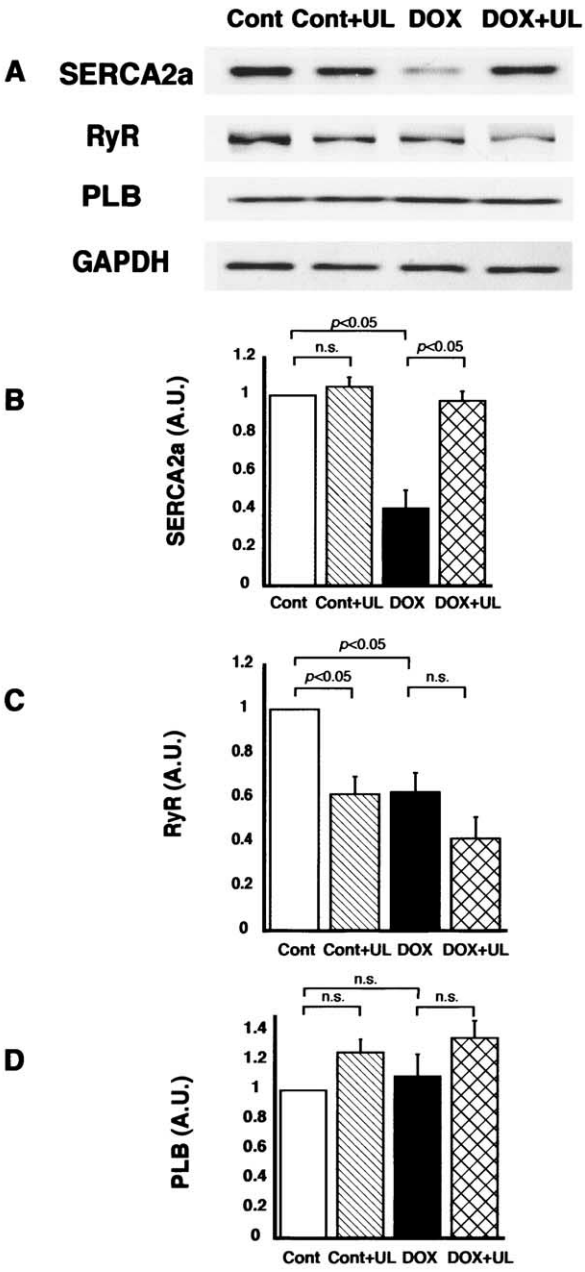

Figure 5. Expression levels of Ca^{2+}-regulatory proteins. **(A)** Representative immunoblots showing the amounts of SERCA2a, RyR, phospholamban (PLB), and GAPDH protein levels in left ventricular (LV) tissues from four groups. The amounts of SERCA2a **(B)**, RyR **(C)**, and PLB **(D)** were quantified by the Odyssey Infrared Imaging System, and the data were normalized to values obtained from LV tissues in the control group. Data represent the mean value ± SEM (Cont, n = 6; Cont+UL, n = 5; DOX, n = 6; DOX+UL, n = 5) A.U. = arbitrary unit; other abbreviations as in Figures 1 and 4.

impaired contractility and $[Ca^{2+}]_i$ transients are improved after mechanical unloading.

Messenger RNA and protein levels of Ca^{2+}-regulatory proteins in LV tissue. To address the mechanisms responsible for recovery of contractility and $[Ca^{2+}]_i$ transient after mechanical unloading in failing cardiomyocytes, we evaluated the mRNA levels of the Ca^{2+}-regulatory proteins (Fig. 4). The levels of SERCA2a mRNA were not changed between control and control+UL. Although the expression of SERCA2a mRNA was depressed in hearts from DOX compared with control, levels had recovered after unloading (DOX+UL). There was no significant difference in the levels of ryanodine receptor (RyR) mRNA among the four groups. The expression levels of both SERCA2a and RyR mRNAs in $Cont_0$ or DOX_0 were similar to those in control or DOX, respectively (data not shown).

The Ca^{2+}-regulatory protein levels in LV tissue. The expression levels of Ca^{2+}-regulatory proteins—SERCA2a, RyR, and PLB—were determined by immunoblotting in LV tissues from the four groups. Doxorubicin treatment decreased the amounts of SERCA2a protein in the DOX_0 by 56% and the DOX by 59% (Figs. 5A and 5B). Mechanical unloading of doxorubicin-treated hearts for two weeks (DOX+UL) increased the amounts of SERCA2a protein to a level comparable to the control, although mechanical unloading did not affect the amounts of SERCA2a protein in control+UL. Doxorubicin treatment also decreased the amounts of RyR protein by 37% (DOX) (Figs. 5A and 5C). Interestingly, mechanical unloading itself decreased the amounts of RyR protein by 38% in control+UL. Mechanical unloading slightly decreased the amounts of RyR protein in doxorubicin-treated hearts (DOX+UL), but the effect was not statistically significant. The amount of PLB protein was not affected either by doxorubicin treatment or mechanical unloading (Figs. 5A and 5D). The amount of GAPDH, a protein unrelated to Ca^{2+} regulation, was similar in all four groups (Fig. 5A), suggesting that the changes in the amounts of SERCA2a and RyR proteins after doxorubicin treatment and/or mechanical unloading were not due to the difference of loaded myocardial tissues. The Western blot analyses confirm that mechanical unloading restores the decreased SERCA2a in doxorubicin-induced cardiomyopathy. Because SERCA2a has a dominant action to stabilize myocardial $[Ca^{2+}]_i$, these data suggest that the ability of $[Ca^{2+}]_i$ uptake into the SR, rather than $[Ca^{2+}]_i$ release from the SR, is probably in deficit in the hearts with doxorubicin-induced cardiomyopathy, and such reduced SERCA2a ability is reversed after mechanical unloading.

Ultrastructural studies. Finally, electron microscopic studies revealed that ultrastructural remodeling, swelling of the SR and mitochondria, and loss of myofibrils were observed in the myocardium from DOX. These ultrastructural changes were similar to a previous report (22). Moreover, ultrastructure of the myocardium from DOX+UL was similar to control, showing a regular myofibrillar arrangement containing dense SR and mitochondria. The ultrastructure of the myocardium from control+UL was similar to that of control (Fig. 6).

DISCUSSION

We demonstrated that mechanical unloading by heterotopic transplantation of the heart with doxorubicin-induced car-

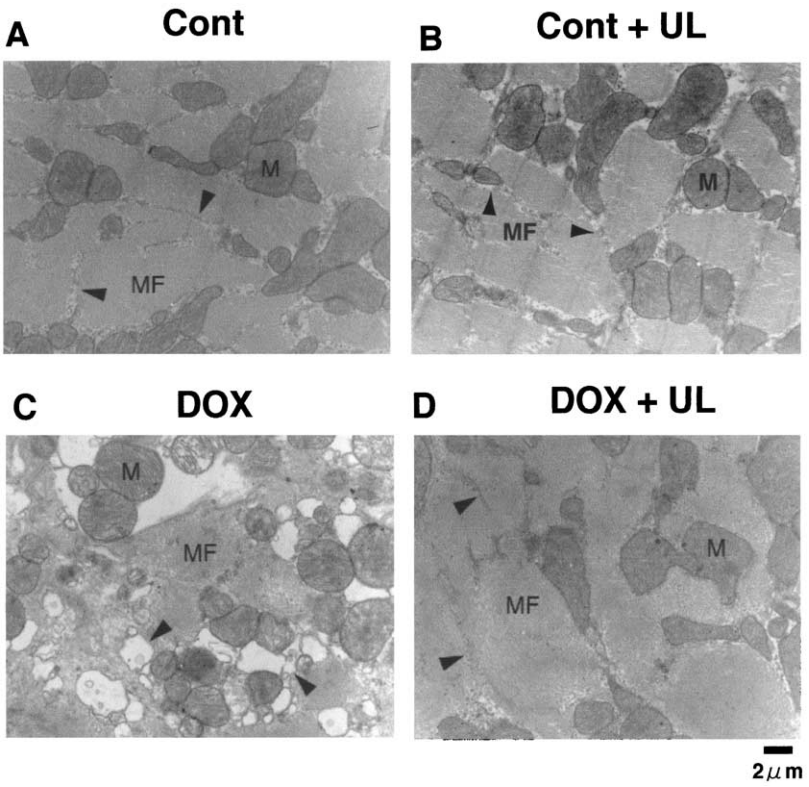

Figure 6. Transmitted electron microscopic images of **(A)** Cont, **(B)** Cont+UL, **(C)** DOX, and **(D)** DOX+UL. In each image, mitochondria (M), myofibrils (MF), and sarcoplasmic reticulum (SR) **(arrowhead)** are indicated. Note the loss of myofibrils and swelling of mitochondria and SR observed in doxorubicin-induced cardiomyopathic cells. Few of these changes could be seen in DOX+UL. Other abbreviations as in Figure 1.

diomyopathy increased SR Ca^{2+} ATPase (SERCA2a), which resulted in improved contractility and intracellular free Ca^{2+} level ($[Ca^{2+}]_i$) dynamics in rats. Human and animal studies are not in agreement with each other concerning the effects of mechanical unloading. This is a novel report, which demonstrates that mechanical unloading has beneficial effects on failing myocardium in small animals. Unloading of the normal animal heart has been reported to have no advantage to the myocardium (9–15). However, there have been successful results with the clinical use of LVADs (1–8) in humans with terminal heart failure; therefore, we focused this study on the effects of unloading in the failing myocardium. We used a doxorubicin-induced cardiomyopathy model in rats to evaluate the effects of unloading in the failing myocardium, because previous studies (16,23) showed a decrease in mRNA expression for SERCA2a protein and impaired $[Ca^{2+}]_i$ handling, and thus reduced cardiac function in this model.

Previous studies (9–15) have demonstrated that mechanical unloading by heterotopic transplantation formed atrophic hearts. The present study showed that the LVW of both unloaded groups with or without doxorubicin treatment was less than DOX or control. Although the LV also weighed less in DOX, the LVW/BW ratio was not different from control, suggesting that doxorubicin did not produce an atrophic heart by itself. All the indexes of both cell shortening and $[Ca^{2+}]_i$ transients in control+UL were unaltered from those of control, except for V_{max}. The levels of RyR proteins were the only significant difference between control and control+UL in mRNA and protein levels of Ca^{2+}-regulatory proteins. A reduced expression of RyR protein could contribute to less mobilization of $[Ca^{2+}]_i$ from the SR at the onset of contraction, and such a decrease in RyR might reduce the V_{max} of $[Ca^{2+}]_i$ transients. The reduction of both mRNA and protein levels of SERCA2a in DOX results in an impaired $[Ca^{2+}]_i$ transient, which contributes to less contraction and slow relaxation of the myocardium. These data are consistent with previous reports (16,23). The insufficient $[Ca^{-2+}]_i$ transient and contractility in doxorubicin-induced cardiomyopathy was improved after mechanical unloading for two weeks, which was accompanied by increases in SERCA2a mRNA and protein levels. Because there was no significant difference in intracellular Ca^{2+} regulatory mRNA and protein levels between DOX and DOX+UL, except for increases in SERCA2a expression, the enhanced intracellular Ca^{2+} uptake into the SR via increased SERCA2a could be responsible for both improved $[Ca^{2+}]_i$ transients and contractility in DOX+UL.

There is another possibility that the improved $[Ca^{2+}]_i$ transients in DOX+UL may enhance activity of the plasma membrane Na^+/Ca^{2+} exchanger and mitochondrial Ca^{2+} uniporter after unloading, although they do not have dominant action on the $[Ca^{2+}]_i$ regulation in myocardium. Ito

et al. (9) and Ritter et al. (15) reported that the Na^+/Ca^{2+} exchanger did not change in the heterotopic heart transplant animal models.

The effects of unloading on the normal heart in this study are consistent with those in previous studies. Thus, mechanical unloading of normal hearts did not provide beneficial effects in contractility, $[Ca^{2+}]_i$ transients, or expression of intracellular Ca^{2+}-regulatory mRNAs and proteins. Ito et al. (9) reported that the protein levels of PLB increased, whereas that of SERCA2a did not change through five weeks of unloading. In our study, unloading of normal hearts for two weeks tended to increase PLB protein levels, whereas the SERCA2a protein levels were not altered.

The present study showed that unloading of the failing heart was beneficial to the Ca^{2+} handling of the heart. Arai et al. (16) reported that doxorubicin increased intracellular H_2O_2 concentration and decreased SERCA2a mRNA levels, which were accompanied by activation of mitogen-activated protein kinases in primary cultures of rat cardiac ventricular myocytes. They have proposed the hypothesis that early growth response-1 and mitogen-activated protein kinases are critical transcriptional factors of the SERCA2a gene. The role of mechanical unloading on the reversal SERCA2a abundance in the failing heart is still unclear.

Conclusions. We have demonstrated that in rats with doxorubicin-induced cardiomyopathy, mechanical unloading can restore contractility and $[Ca^{2+}]_i$ regulation via recruiting functional SERCA2a. It is possible to elucidate the involvement of the SERCA2a regulatory pathway and $[Ca^{2+}]_i$ regulation in pathophysiologic states using this model.

Acknowledgments

We thank Professor Hideho Higashi and Associate Professor Eiichiro Tanaka for encouragement for this study. We also thank Dr. Junichi Honda and Dr. Hiroharu Mifune, Ms. Yumi Yokose, Dr. Masaru Nishimi, Dr. Shuji Fukunaga, Dr. Shizuka Iida, Ms. Satoko Yamada, and Ms. Mayumi Oyabu for their technical assistance. We are grateful to Professor Eiichi Kumamoto, Dr. Takao Shioya (Saga University), and Dr. Masamichi Ono (Osaka University) for their technical support. We thank Dr. Tomoe Y. Nakamura and Dr. Yoritaka Otsuka (National Cardiovascular Center) for the helpful discussion and critical evaluation of the manuscript.

Reprint requests and correspondence: Dr. Tohru Takaseya, Department of Surgery, Kurume University School of Medicine, 67 Asahi-machi, Kurume 830-0011, Japan. E-mail: takaseya@med.kurume-u.ac.jp.

REFERENCES

1. Frazier OH, Myers TJ. Left ventricular assist system as a bridge to myocardial recovery. Ann Thorac Surg 1999;68:734–41.
2. Bartling B, Milting H, Schumann H, et al. Myocardial gene expression of regulators of myocyte apoptosis and myocyte calcium homeostasis during hemodynamic unloading by ventricular assist devices in patients with end-stage heart failure. Circulation 1999;100 Suppl II:II-216–23.
3. Dipla K, Mattiello JA, Jeevanandam V, Houser SR, Margulies KB. Myocyte recovery after mechanical circulatory support in humans with end-stage heart failure. Circulation 1998;97:2316–22.
4. Heerdt PM, Holmes JW, Cai B, et al. Chronic unloading by left ventricular assist device reverses contractile dysfunction and alters gene expression in end-stage heart failure. Circulation 2000;102:2713–9.
5. Ogletree-Hughes ML, Stull LB, Sweet WE, Smedira NG, McCarthy PM, Moravec CS. Mechanical unloading restores beta-adrenergic responsiveness and reverses receptor downregulation in the failing human heart. Circulation 2001;104:881–6.
6. Park SJ, Zhang J, Ye Y, et al. Myocardial creatine kinase expression after left ventricular assist device support. J Am Coll Cardiol 2002;39:1773–9.
7. de Jonge N, van Wichen DF, Schipper ME, et al. Left ventricular assist device in end-stage heart failure: persistence of structural myocyte damage after unloading. An immunohistochemical analysis of the contractile myofilaments. J Am Coll Cardiol 2002;39:963–9.
8. Blaxall BC, Tschannen-Moran BM, Milano C, Koch WJ. Differential gene expression and genomic patient stratification following left ventricular assist device support. J Am Coll Cardiol 2003;41:1096–106.
9. Ito K, Nakayama M, Hasan F, Yan X, Schneider MD, Lorell BH. Contractile reserve and calcium regulation are depressed in myocytes from chronically unloaded hearts. Circulation 2003;107:1176–82.
10. Klein I, Samarel AM, Welikson R, Hong C. Heterotopic cardiac transplantation decreases the capacity for rat myocardial protein synthesis. Circ Res 1991;68:1100–7.
11. Depre C, Shipley GL, Chen W, et al. Unloaded heart in vivo replicates fetal gene expression of cardiac hypertrophy. Nat Med 1998;4:1269–75.
12. Korecky B, Ganguly PK, Elimban V, Dhalla NS. Muscle mechanics and Ca^{2+} transport in atrophic heart transplants in rat. Am J Physiol 1986;251:H941–8.
13. Kolár F, MacNaughton C, Papourek F, Korecky B, Rakusan K. Changes in calcium handling in atrophic heterotopically isotransplanted rat heart. Basic Res Cardiol 1995;90:475–81.
14. Rakusan K, Heron MI, Kolar F, Korecky B. Transplantation-induced atrophy of normal and hypertrophic rat hearts: effect on cardiac myocytes and capillaries. J Mol Cell Cardiol 1997;29:1045–54.
15. Ritter M, Su Z, Xu S, Shelby J, Barry WH. Cardiac unloading alters contractility and calcium homeostasis in ventricular myocytes. J Mol Cell Cardiol 2000;32:577–84.
16. Arai M, Yoguchi A, Takizawa T, et al. Mechanism of DOX-induced inhibition of sarcoplasmic reticulum Ca^{2+}-ATPase gene transcription. Circ Res 2000;86:8–14.
17. Suzuki K, Murtuza B, Suzuki N, Smolenski RT, Yacoub MH. Intracoronary infusion of skeletal myoblasts improves cardiac function in DOX-induced heart failure. Circulation 2001;104 Suppl I:I213–7.
18. Siveski-Iliskovic N, Hill M, Chow DA, Singal PK. Probucol protects against adriamycin cardiomyopathy without interfering with its antitumor effect. Circulation 1995;91:10–5.
19. Ono K, Lindsey ES. Improved technique of heart transplantation in rats. J Thorac Cardiovasc Surg 1969;57:225–9.
20. Yamamoto S, Ehara T, Shioya T. Changes in cell volume induced by activation of the cyclic AMP-dependent chloride channel in guinea-pig cardiac myocytes. Jpn J Physiol 2001;51:31–41.
21. Straub B, Müller M, Krause H, et al. Detection of prostate-specific antigen RNA before and after radical retropubic prostatectomy and transurethral resection of the prostate using 'Light-Cycler'-based quantitative real-time polymerase chain reaction. Urology 2001;58:815–20.
22. Signal PK, Segstro RJ, Singh RP, Kutryk MJ. Changes in lysosomal morphology and enzyme activities during the development of adriamycin-induced cardiomyopathy. Can J Cardiol 1985;1:139–47.
23. Arai M, Tomaru K, Takizawa T, et al. Sarcoplasmic reticulum genes are selectively down-regulated in cardiomyopathy produced by DOX in rabbits. J Mol Cell Cardiol 1998;30:243–54.